

## Interpretation of Mirnov Measurements in ASDEX Upgrade

M. Schittenhelm, H. Zohm, ASDEX Upgrade - Team

Max-Planck-Institut für Plasmaphysik - EURATOM Association, D-85740 Garching

Most MHD instabilities are connected with perturbations of the equilibrium field. The evaluation of the perturbation field would be one of the directest methods to investigate the mode structure. Unfortunately, in a hot fusion plasma, measurements of the perturbation fields using pick-up coils (Mirnov probes) [1] are only possible outside the plasma without any resolution in the radial direction. Due to this reason, the analysis of complex mode structures is difficult.

In the ASDEX Upgrade tokamak [2], the modulation of the poloidal field due to a rotating mode structure is measured by a poloidal array of 30 pick-up coils and by 4 coils in a toroidal plane. For a detailed analysis of the modes, the Mirnov probe measurements are compared with simulations of the perturbation field at the probe locations. In the simulation, the current flows along the equilibrium field lines on the resonant flux surface and, to ensure  $\nabla \cdot \mathbf{j} = 0$ , the current density is proportional to the magnetic field. The location of the resonant surface and the field line geometry are computed from equilibrium analysis. The induced screening currents in vacuum vessel and in conducting structures close to the Mirnov probes are taken into account while computing the perturbation field. Results of this new Mirnov Interpretation Code (MIC) are presented in the following section.

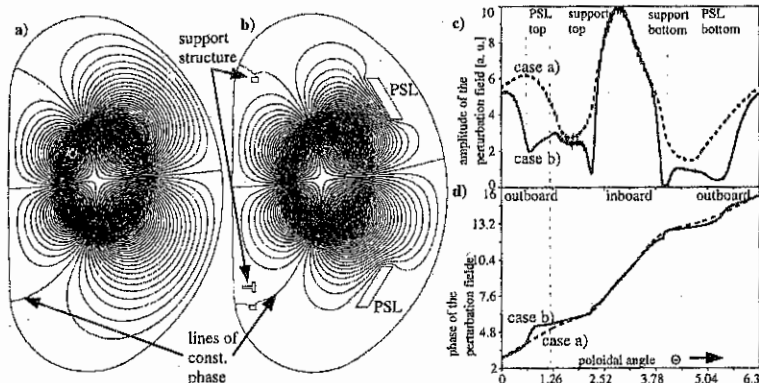


Figure 1: Influence of the screening currents on the perturbation field. a) Simulation of the perturbation flux for a typical  $m=2$  mode considering screening currents only in the vessel. b) Simulation with additional screening currents of in-vessel components. c), d) Amplitude and phase of the perturbation field parallel to the vessel at the probe position (2.5 cm inside the vessel) in the cases a and b.

For the discussion of the influence of the screening currents, Fig. 1 shows the computed perturbation flux function, which results from an  $m = 2$  perturbation on the  $q = 2$

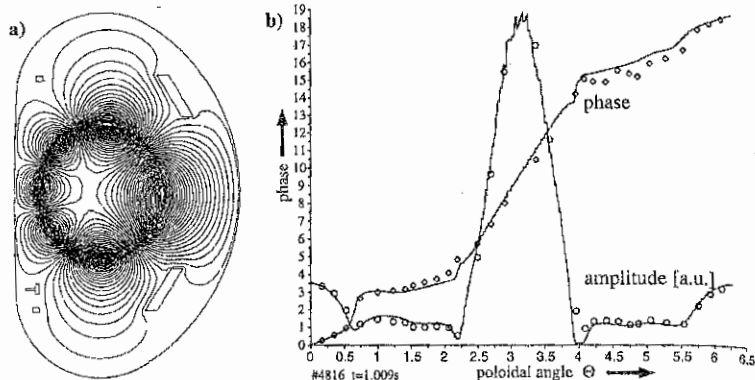


Figure 2: Comparison of the calculation and the measurements of a  $m = 3$  mode in a limiter plasma with circular cross-section. a) Calculated perturbation flux. b) The amplitude and the phase of the mode vs. the poloidal angle of the probe position. The simulated perturbation field is in good agreement with the measurements.

surface (the edge  $q$  of the plasma is  $q_{95} = 5.0$ ). Due to screening currents, the flux function vanishes at the vessel wall and the contour lines nestle to the wall. The phase at a given poloidal angle  $\Theta$  depends on the radial distance from the resonant surface. Points of equal phase can be found along the lines of vanishing flux (Fig. 1a). Away from the midplane, points of equal phase have a clear divergence from a straight line. Ignoring this 'vessel effect', the reduction of the wave length on the high field side due to toroidicity, shaping and  $\beta$ -effects would be overestimated.

Fig. 1c,d shows the influence of the in-vessel components on the perturbation fields. The amplitude and phase are computed 2.5 cm inside the vessel (position of the Mirnov probes) versus the poloidal angle  $\Theta$ . Close to the in-vessel components, the screening effect reduces the amplitude up to a factor of 10. The amplitude in the midplane shows a small influence. The influence on the phase is only noticeable outboard in the region of the Passive Stabilisation Loop (PSL) which is formed like a saddle coil ( $m=1$ ;  $n=0$  structure) to slow down the vertical plasma movement [3]. Together with their support structure, the conductors of the PSL result in an effective  $n=8$  screening loop in front of the outboard probes at usual mode frequencies of several kHz.

The new method for the interpretation of Mirnov measurements can be demonstrated for a circular limiter plasma in a fast current ramp up scenario. Due to the decreasing edge safety factor  $q$ , a ( $m = 3$ ,  $n = 1$ ) kink mode can develop when the  $q = 3$  surface leaves the plasma. The simulation assuming a perturbation current on this surface shows a good agreement with the measurements (Fig. 2).

On the contrary to the circular limiter plasma discussed before, a dominant ( $m = 2$ ,  $n = 1$ ) mode always occurs before disruptions in elongated divertor plasmas. In this case, the simulated amplitude of the modulation is in disagreement with the measurements. The measured and simulated ratio between the amplitudes of outboard and inboard midplane probes differs by a factor of two. Another experimental fact is that the ratio between these

amplitudes is not constant during the growth of the modes. Especially in a density limit discharge with high  $q_{95} = 5$  at the edge, the amplitude of the perturbation field increases by a factor of 10 in a few ten milliseconds before the first minor disruption. In this short time interval, the equilibrium of the plasma does not change, but the ratio between the inside and the outside amplitude decreases, as shown in Fig. 3a. The variation of the

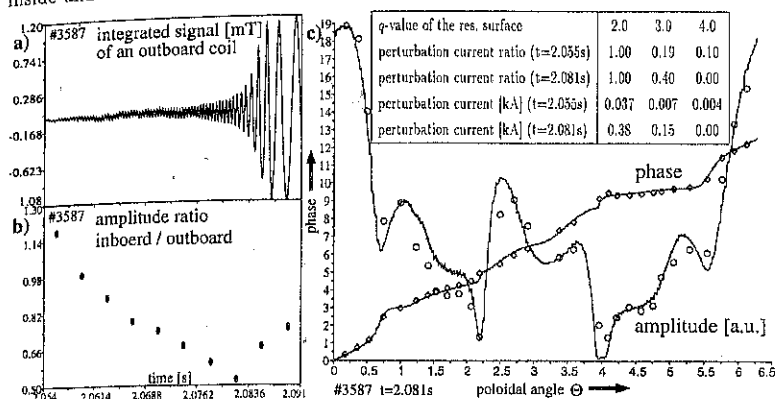


Figure 3: Before the density limit is reached, a MHD mode develops. a) In the high  $q$  case, the amplitude increases by a factor of 10 in few ten milliseconds. b) The measured amplitude of the low field side increases more than two times faster compare to the high field side although there is no change of the position or the equilibrium of the plasma. By assuming mode coupling, the simulation fits the measurements very well.

amplitude ratio indicates the development of coupled modes on neighbouring resonant surfaces. Assuming perturbation currents on those surfaces, the perturbation field is computed for every surface alone in the described way. To superpose the fields for the final result, it is necessary to find the correct ratio between the perturbation currents on the different surfaces. Using complex amplitudes for the specification of the simulated and measured field (i. e. also allowing for a varying phase angle), the value of the currents on the different surfaces can be computed by a least square fit. To get a good agreement with the measurements in the case shown in Fig. 3c, perturbation currents are assumed on the  $q = 2$ ,  $q = 3$  and  $q = 4$  surfaces. The amplitudes of the assumed sheet currents are summarised in Fig. 3c for two time points at the begin and the end of the mode growth. Comparing the two time points, it becomes clear that the coupled  $m = 3$  mode grows twice as fast as the dominant  $m = 2$  mode. In spite of the strong contribution of the  $m = 3$  mode at  $t = 2.081$ s, the phase is dominated by the  $m = 2$  mode. Only the consideration of the amplitude and phase can give the contribution of coupled modes in the presented way.

Fig. 4a shows the time traces of a representative, high  $q$  density limit discharge ( $q_{95} = 5$ ) [4] 150 ms before the final disruption. Approximately 10 ms before the density limit, a rotating MHD-mode occurs and grows exponentially. The rotation frequency decreases from 2.4 kHz to 0.72 kHz at the saturation point. At first, no mode locking occurs

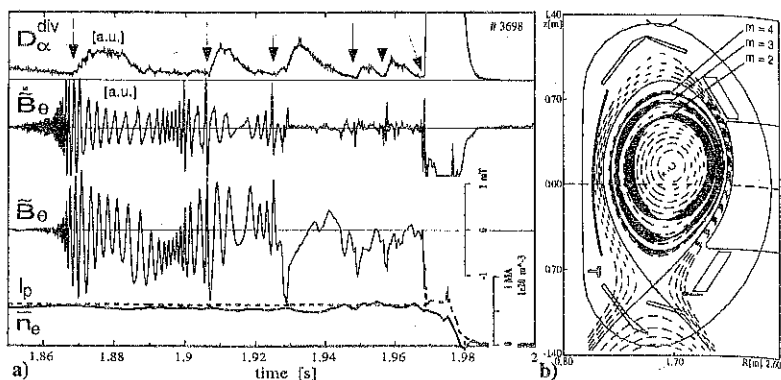


Figure 4: a) Time traces of a density limit discharge at high  $q$ . The arrows mark the begin of an increased transport of particles and energy on the divertor plate at the occurrence of a minor disruption or the terminating major disruption. b) The reconstructed island structure at  $t=1.869$ s

and the islands decrease their amplitudes. At lower amplitude, the islands accelerate their rotation until the perturbation increases again. The islands saturate at the same amplitude as before. This cycle is repeated two or three times until the mode locks. After 30 to 50 ms the major disruption terminates the discharge.

Using the analysis presented before, the saturation amplitudes of perturbation currents are ( $t=1.869$ s):  $q=2$ : 4.3kA;  $q=3$ : 1.9kA;  $q=4$ : 0.43kA. By superposing the helical equilibrium flux and the computed perturbation flux, the resulting islands can be illustrated. Although this linear treatment does not give the new consistent equilibrium with all perturbation currents, it allows to illustrate the island structure and to give an estimate for the island width (Fig. 4b). This analysis confirms that the minor disruptions start when the growing islands on the different surfaces come close together [5, 6]. Because of the mode locking before the major disruption such an exact analysis of the measurements is not possible for the major disruption.

To summarize, it should be pointed out that the phase and amplitude of the perturbation field must be considered to reconstruct complex mode structures. By a comparison of the simulated perturbation field with the measurement, the contribution of coupled modes on different surfaces and of the induced screening currents can be distinguished. The induced screening currents have a noticeable influence on the measured perturbation field.

## References

- [1] S. Mironov and I.V. Semenov. *Plasma Phys. Contr. Fusion Research*, 2:22, 1971.
- [2] W. Köppendörfer et. al. In *Fourteenth international conference on plasma physics and controlled nuclear fusion research, Würzburg, Germany*. IAEA, Wien, 1992.
- [3] O. Gruber et al. *Plasma Phys. Contr. Fusion*, 35:B191, 1993.
- [4] V. Mertens et al. *Plasma Phys. Contr. Fusion*, 36:1307, 1994.
- [5] A. Bondeson et. al. *Nuclear Fusion*, 31:1695, 1991.
- [6] H. Zohm et al. *Plasma Phys. Contr. Fusion*, 37:A313, 1995.